

## Lateral Diffusion on Fused Cell Doublets

Dear Sir:

The measurement of surface intermixing rates on fused cell doublets has long been used to estimate lateral diffusion coefficients in membranes (1-7). This method could become particularly attractive now with the recent introduction of electric pulse fusion techniques (7). Nevertheless, the problem of diffusion on the double-lobed surface of fused cell pairs (Fig. 1), the characteristic shape of fused erythrocytes (2-7), appears to have not been solved except in the limiting case of a spherical surface (8). This problem is, in fact, formally identical to another problem that has been solved: the diffusion-mediated trapping into a circular region on the surface of a sphere. Recent articles by Chao et al. (9) and Weaver (10) have analyzed this latter problem as a possible model for the localization of mobile cell surface components induced by local surface modulation.

Fig. 1 illustrates the equivalence of the two problems: diffusion to a perfect trap on a single cell (left side) and intermixing on a symmetrical fused doublet (right side). Concentrations are initially uniform functions of equatorial angle  $\theta$ :  $c(\mu \equiv \cos \theta, 0) = c_0$  for the single cell and the labeled fused cell, and  $c(\mu, 0) = 0$  for the unlabeled fused cell. For the single cell, the boundary condition  $c(\mu_0, t) = 0$ , for all  $t > 0$ , establishes the hatched region,  $\mu \leq \mu_0 \equiv \cos \theta_0$ , as a perfect concentration sink (9, 10). For the fused pair, simple symmetry considerations maintain  $c(\mu, t) = c_0/2$  for all  $t > 0$ . Thus,  $2c(\mu, t) - c_0$  for the labeled fused cell and  $c_0 - 2c(\mu, t)$  for the unlabeled fused cell are identical to  $c(\mu, t)$  on the single cell for all  $\mu \geq \mu_0$ .

Adapting the results of Chao et al. (9),  $|2c(\mu, t) - c_0|$  can be

written as a sum of nonintegral Legendre functions (11). For molecules diffusing with diffusion coefficient  $D$ ,

$$|2c(\mu, t) - c_0| = \sum_{s=0}^{\infty} A_s P_s(\mu) \exp(-k_s^2 D t), \quad (1)$$

where  $\nu_s (s = 0, 1, 2, \dots)$  are successive real numbers (tabulated and graphed in reference 11) for which  $P_{\nu_s}(\mu)$  vanishes at  $\mu = \mu_0$ , and

$$k_s^2 = \nu_s(\nu_s + 1)/R_0^2. \quad (2)$$

For a sphere (i.e.,  $\mu_0 = 0$ ),  $\nu_s$  reduces to the series of odd integers. Experimentally, one can apply the normal-mode analysis (5, 12, 13) to compute experimental estimates of  $k_0^2 D$  and hence  $D$  if  $k_0^2$  is known.

Alternatively, adapting the results of Weaver (10), the intermixing after fusion can be analyzed in terms of a mean transfer time:

$$\tau \equiv \int_0^{\infty} [\Delta c(t)/\Delta c(0)] dt = \frac{R_0^2}{D} \left[ \frac{2}{1 - \mu_0} \ln \left( \frac{2}{1 + \mu_0} \right) - 1 \right], \quad (3)$$

where  $\Delta c(t)$  is the average concentration difference between the originally labeled and unlabeled cells. Except at very short times ( $t \ll \tau$ ),  $\Delta c(t)$  approximates a single exponential (10):

$$\Delta c(t) \approx \Delta c(0) e^{-k^2 D t}, \quad (4a)$$

where

$$k^2 = 1/D\tau. \quad (4b)$$

Given experimental values of  $\tau$ , one can calculate  $D$  if  $k^2$  is known.

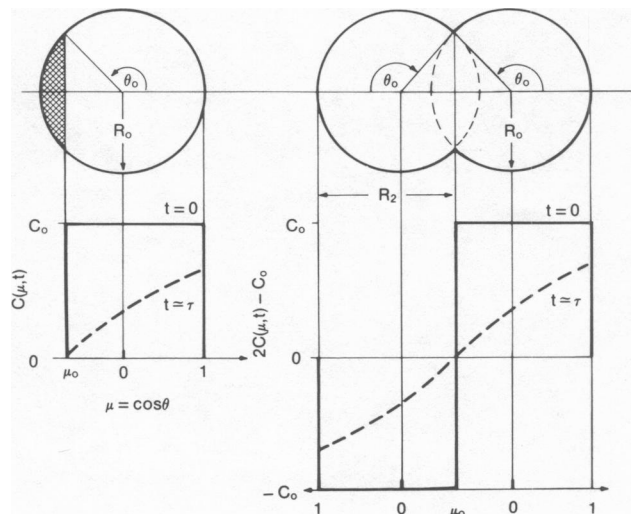


FIGURE 1 Geometries (top) and surface concentration distributions (bottom) for the diffusion to a perfect trap on the surface of a single spherical cell (left) and the diffusion-mediated intermixing on a symmetrical fused cell doublet (right). As indicated, the solid straight lines are initial concentration distributions. The dashed curves approximate the concentration distribution after about one characteristic time constant.

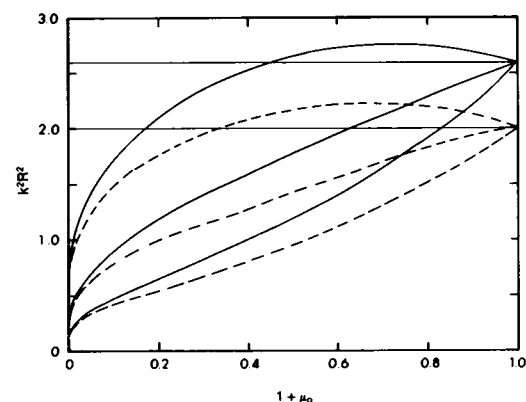


FIGURE 2 Dimensionless characteristic intermixing rates as functions of  $1 + \mu_0$ . The dashed curves trace out  $k_0^2 R_0^2$  (bottom),  $k_0^2 R_1^2$  (middle), and  $k_0^2 R_2^2$  (top). The solid curves trace out  $k^2 R_0^2$  (bottom),  $k^2 R_1^2$  (middle), and  $k^2 R_2^2$  (top).  $1 + \mu_0$  spans the range of values from that corresponding to two separate spheres ( $1 + \mu_0 = 0$ ) to that for a single spherical fused product ( $1 + \mu_0 = 1$ ).

In the absence of more exact solutions, previous studies (2–4, 6, 7) have analyzed diffusion rates on fused doublets in terms of effective equivalent spheres: spheres of radius  $R_1$  adjusted to give the same surface area as the fused doublet (2, 3, 6, 7); and spheres of radius  $R_2$  (Fig. 1) equal to half the actual long dimension (4). In terms of  $R_0$  and  $\mu_0$ .

$$R_1 = (1 - \mu_0)^{1/2} R_0 \quad (5a)$$

$$R_2 = (1 - \mu_0) R_0. \quad (5b)$$

Given the results above, we can test the accuracy of these intuitive approaches.

Fig. 2 represents theoretical values of  $k_0^2 R_0^2$ ,  $k_0^2 R_1^2$ ,  $k_0^2 R_2^2$ ,  $k^2 R_0^2$ ,  $k^2 R_1^2$ , and  $k^2 R_2^2$  as functions of  $1 + \mu_0$ , calculated according to Eqs. 2–5 and the tables and graphs in reference 11. Each curve traces the variation of the intermixing rate as  $\theta_0$  is varied but the corresponding radius ( $R_0$ ,  $R_1$ , or  $R_2$ ) is kept constant. Choosing  $R_1$  or  $R_2$  as the radius of effective spheres is equivalent to assuming that, at the actual value of  $\theta_0$  for a given fused doublet,  $k_0^2 R_1^2$  and  $k^2 R_1^2$ , or  $k_0^2 R_2^2$  and  $k^2 R_2^2$  do not differ appreciably from their values for a sphere (the horizontal straight lines in Fig. 2). It is thus seen that  $R_2$  is significantly better than  $R_1$  as an effective radius, giving results accurate to within 10% for  $1 + \mu_0 > 0.3$ . The use of either, however, will lead to significant underestimates of  $D$  to various degrees for values of  $1 + \mu_0$  much below 0.3. In the future, the results of Chao et al. (9) and Weaver (10) can be adapted as above and used for exact analyses.

Received for publication 11 June 1984.

## REFERENCES

1. Frye, L. D., and M. Edidin. 1970. The rapid intermixing of cell surface antigens after formation of mouse-human heterokaryons. *J. Cell. Sci.* 7:319–335.

2. Fowler, V., and D. Branton. 1977. Lateral mobility of human erythrocyte integral membrane proteins. *Nature (Lond.)* 268:23–26.
3. Fowler, V., and V. Bennett. 1978. Association of spectrin with its membrane attachment site restricts lateral mobility of human erythrocyte integral membrane proteins. *J. Supramol. Struct.* 8:215–221.
4. Schindler, M., D. E. Koppel, and M. P. Sheetz. 1980. Modulation of membrane protein lateral mobility by polyphosphates and polyamines. *Proc. Natl. Acad. Sci. USA* 77:1457–1461.
5. Koppel, D. E., and M. P. Sheetz. 1981. Fluorescence photobleaching does not alter the lateral mobility of erythrocyte glycoproteins. *Nature (Lond.)* 293:159–161.
6. Smith, D. K., and J. Palek. 1982. Modulation of lateral mobility of band 3 in the red cell membrane by oxidative cross-linking of spectrin. *Nature (Lond.)* 297:424–425.
7. Sowers, A. E. 1984. The lateral diffusion of Dil from a labeled membrane to an unlabeled membrane following electric field induced fusion: a new quantitative technique. *Biophys. J.* 45 (2, Pt. 2):331a. (Abstr.)
8. Huang, H. W. 1973. Mobility and diffusion in plane of cell membrane. *J. Theor. Biol.* 40:11–17.
9. Chao, N.-m., S. H. Young, and M.-m. Poo. 1981. Localization of cell membrane components by surface diffusion into a "trap." *Biophys. J.* 36:139–153.
10. Weaver, D. L. 1983. Diffusion-mediated localization on membrane surfaces. *Biophys. J.* 41:81–86.
11. Hall, R. N. 1949. The application of non-integral Legendre functions to potential problems. *J. Appl. Phys.* 20:925–936.
12. Koppel, D. E., M. P. Sheetz, and M. Schindler. 1980. Lateral diffusion in biological membranes: a normal-mode analysis of diffusion on a spherical surface. *Biophys. J.* 30:187–192.
13. Koppel, D. E. 1985. Normal-mode analysis of lateral diffusion on a bounded membrane surface. *Biophys. J.* In press.

DENNIS E. KOPPEL, *Department of Biochemistry, University of Connecticut Health Center, Farmington, Connecticut 06032*